



# Competition for synchronization in a phase oscillator system



Yakov Kazanovich<sup>a</sup>, Oleksandr Burylko<sup>b</sup>, Roman Borisyuk<sup>c,a,\*</sup>

<sup>a</sup> Institute of Mathematical Problems of Biology, Russian Academy of Sciences, 142290 Pushchino, Russia

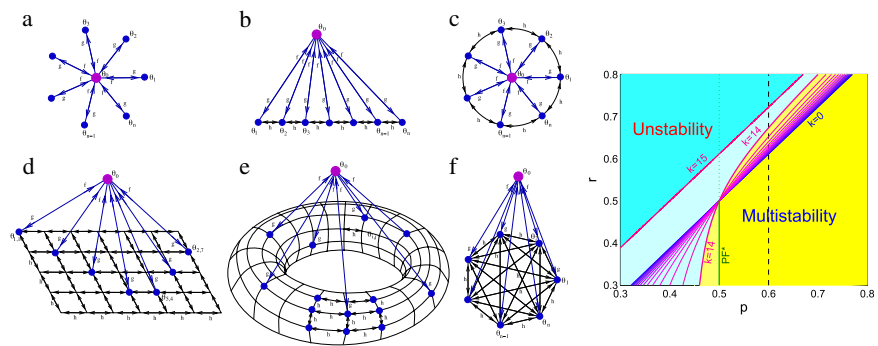
<sup>b</sup> Institute of Mathematics, National Academy of Sciences of Ukraine, Tereshchenkivska Str. 3, 01601 Kyiv, Ukraine

<sup>c</sup> School of Computing and Mathematics, University of Plymouth, Plymouth, PL4 8AA, UK

## HIGHLIGHTS

- A system of general phase oscillators interacting in a star-like manner is studied.
- Analytical descriptions of stability are given.
- Multistability, heteroclinic orbits, and chaos are possible.
- The application of the results to modeling in neuroscience is discussed.

## GRAPHICAL ABSTRACT



## ARTICLE INFO

### Article history:

Received 23 March 2013

Received in revised form

3 July 2013

Accepted 7 July 2013

Available online 15 July 2013

Communicated by S. Coombes

### Keywords:

Coupled oscillators

Kuramoto model

Networks with a central element

Bifurcations

## ABSTRACT

A system of phase oscillators with a Central Oscillator (CO) and a set of  $n$  Peripheral Oscillators (POs) is considered. Feed-forward and feedback connections between the CO and POs are determined by two interaction functions which are assumed to be smooth, odd, and periodic. To describe the competition of POs for synchronization with the CO, we study the asymptotic stability of fixed points corresponding to in-phase synchronization of a group of  $k$  POs, while other POs are in anti-phase with the CO. It is shown that stability conditions can be formulated in terms of four parameters that describe the slopes of the interaction functions at zero and half-period points. Analytical description of stability in terms of the regions in 4-dimensional parameter space is given. Combining stability analysis with the detailed study of geometry of invariant manifolds, the bifurcations of fixed points are investigated. We show that various dynamical regimes such as multistability, heteroclinic orbits, and chaos are possible. Analytical stability conditions for global synchronization of POs with the CO are formulated for the systems with local connections between POs. It is shown that synchronization in a large system with local connections becomes unstable even under weak desynchronizing influence from the CO. The application of the results to modeling in neuroscience and, in particular, for modeling visual attention is discussed.

© 2013 Elsevier B.V. All rights reserved.

## 1. Introduction

Many systems in physics, chemistry and biology can be modeled by coupled phase oscillators of the Kuramoto type [1]. A review of the mathematical theory of phase oscillator networks

and their applications can be found in the papers [2–5]. We consider a special type of phase oscillator systems, the so-called networks with a central unit. In the networks with a central unit global interaction is realized through a central oscillator (CO) that has feedforward and feedback connections with all the other oscillators that are called peripheral oscillators (PO). Besides connections with the CO peripheral oscillators may optionally have local connections with their neighbors. Various types of connection architectures of networks with a CO are shown in Fig. 1. The architecture in Fig. 1(a) is known as the star-coupled system.

\* Corresponding author at: School of Computing and Mathematics, University of Plymouth, Plymouth, PL4 8AA, UK.

E-mail address: [rborisjuk@plymouth.ac.uk](mailto:rborisjuk@plymouth.ac.uk) (R. Borisyuk).

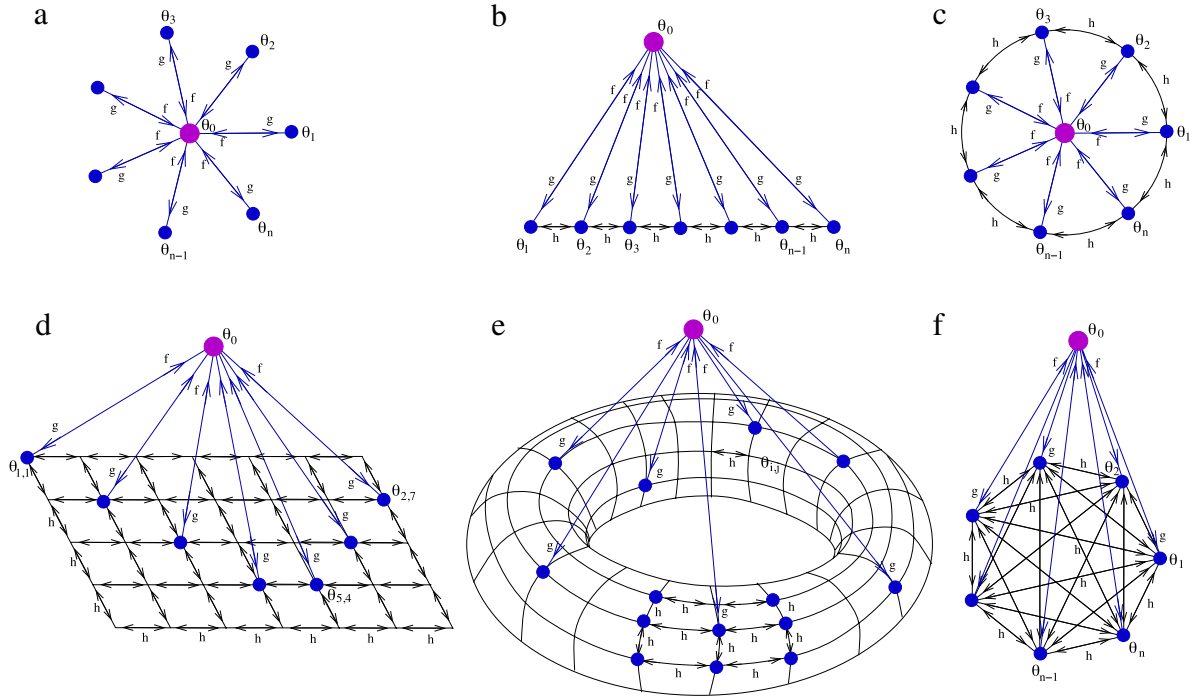


**Fig. 1.** Different types of connections between the CO and POs: (a) star-like connections (without local interaction between POs), (b) POs are arranged in a line, each PO couples with its nearest left and right neighbors, (c) POs are coupled on a circle, (d) POs locate in the nodes of a two-dimensional square grid, each PO couples with its nearest neighbors at left, right, top, and bottom, (e) POs locate on the surface of a torus, (f) global connections between POs.

Fig. 1(b)–(e) present different types of connection architectures with local coupling between POs.

Networks with a central unit appear as parts of more complex networks in so different fields as communication systems, social networks, and mammalian brains. In the latter case they are widely spread due to convergent organization of connections in the hierarchy of brain structures [6,7]. The study of star-coupled systems can be helpful in clearing up the role of synchronization in cognitive functions. Phase oscillator models provide a convenient and mathematically tractable instrument for this study.

Though the dynamics of phase oscillator networks with a central unit (or their equivalent representation in the form of phase differences, see Eqs. (3) below) has been studied in a number of papers [8–19], the analysis of stable states in such systems is far from being complete. In this paper we concentrate on the stability of the regime when POs compete for the synchronization with the CO and only  $k$  POs can be synchronized with the CO while other  $(n - k)$  POs work in anti-phase. (A particular case when  $k = 1$  can be considered as an oscillatory analogue of a winner-take-all procedure.)

Though we use standard linear analysis of fixed points, the effect of competition for synchronization between POs was not obvious from the beginning. For the Kuramoto system with all-to-all connections in-phase/anti-phase relations can be obtained in two assemblies of oscillators receiving synchronizing (the conformist assembly) and desynchronizing (the contrarian assembly) connections [20]. In the system with a CO the set of POs can be split into two mutually anti-phase assemblies despite the uniform influence on POs from the CO. Moreover, simple analytical description of parameter regions corresponding to this regime allows one to construct a system with particular in-phase/anti-phase relations in oscillator activity. The results are applied to understand the mechanism of transitions between different dynamical regimes under the variation of parameters, in particular, the transitions between stability and instability of different types of the regimes of competition. Conditions of multistability in the system are studied that

allow one to describe the parameter regions where a given set of stable states is present.

We also investigate the stability of the in-phase state in a system with local connections between POs and show that this state can be destroyed under a weak desynchronizing influence of the CO if the size of the network is large enough.

## 2. A system without local connections between peripheral oscillators

In this section we consider a star-coupled phase oscillator system (Fig. 1(a)). Let us index the oscillators by numbers  $i = 0, 1, \dots, n$ , where 0 corresponds to the CO and  $1, \dots, n$  correspond to POs. We consider a system whose dynamics is described by the following ODEs:

$$\frac{d\theta_0}{dt} = \omega_0 + \sum_{i=1}^n f(\theta_i - \theta_0), \quad (1)$$

$$\frac{d\theta_i}{dt} = \omega_i + g(\theta_0 - \theta_i), \quad i = 1, \dots, n, \quad (2)$$

where  $(\theta_0, \theta_1, \dots, \theta_n) \in \mathbb{T}^{n+1}$  are phase variables on a  $(n + 1)$ -dimensional torus,  $\theta_i \in [0, 2\pi)$ ,  $\omega_i$  are the natural frequencies of the oscillators,  $f(x), g(x)$  are interaction functions. The interaction functions are odd, continuous,  $2\pi$ -periodic. It follows from these assumptions that

$$f(0) = f(\pi) = g(0) = g(\pi) = 0.$$

Subtracting Eq. (1) from Eq. (2) we get

$$\frac{d\varphi_i}{dt} = \Delta_i - \sum_{j=1}^n f(\varphi_j) - g(\varphi_i), \quad i = 1, \dots, n, \quad (3)$$

where  $\varphi_i = \theta_i - \theta_0$ ,  $\Delta_i = \omega_i - \omega_0$ . We restrict the consideration of system (3) to the case when all oscillators have identical natural frequencies

$$\omega_i = \omega, \quad i = 0, \dots, n,$$

therefore we put  $\Delta_i = 0$  in (3). Denote

$$f'(0) = a_1, \quad f'(\pi) = a_2, \quad g'(0) = b_1, \quad g'(\pi) = b_2. \quad (4)$$

The values in (4) will be used as the parameters of the system.

The case  $n = 1$  is well known, therefore below we always assume that  $n \geq 2$ .

### 3. Stable points

The points  $\Phi = (\varphi_1, \dots, \varphi_n)$  with coordinates  $\varphi_i \in \{0, \pi\}$  ( $i = 1, \dots, n$ ) are fixed points of system (3) (other fixed points can also exist). Our nearest task is to study the asymptotic stability of a point  $\Phi_k$  with  $k$  coordinates equal to 0, and  $(n - k)$  coordinates equal to  $\pi$ . Due to symmetry, for a fixed  $k$  all such points have the same type of stability. Linearizing system (3) we can determine eigenvalues for the point  $\Phi_k$ :

$$k = 0 : \lambda_{1, \dots, n-1} = -b_2, \quad \lambda_n = -na_2 - b_2; \quad (5)$$

$$k = 1 : \lambda_{1, \dots, n-2} = -b_2 \quad (\text{if } n \geq 3),$$

$$\lambda_{n-1, n} = z; \quad (6)$$

$$2 \leq k \leq n - 2 : \lambda_{1, \dots, k-1} = -b_1,$$

$$\lambda_{k, \dots, n-2} = -b_2, \quad \lambda_{n-1, n} = z; \quad (7)$$

$$k = n - 1 : \lambda_{1, \dots, n-2} = -b_1 \quad (\text{if } n \geq 3),$$

$$\lambda_{n-1, n} = z; \quad (8)$$

$$k = n : \lambda_{1, \dots, n-1} = -b_1, \quad \lambda_n = -na_1 - b_1, \quad (9)$$

where

$$z = -z_1 \pm \sqrt{z_2^2 + z_3}, \quad (10)$$

$$z_1 = \frac{na_2 + k(a_1 - a_2) + (b_1 + b_2)}{2}, \quad (11)$$

$$z_2 = \frac{-na_2 + k(a_1 + a_2) + (b_1 - b_2)}{2}, \quad (12)$$

$$z_3 = k(n - k)a_1a_2. \quad (13)$$

Note that for the brevity of notation in formulas (6)–(8) a single variable  $z$  is used to denote two different values determined by (10).

According to (10)–(13) the variables  $z, z_1, z_2, z_3$  depend on the parameters  $n, k, a_1, a_2, b_1, b_2$ , therefore the conditions of stability for a point  $\Phi_k$  can be formulated in terms of inequalities on relations between these parameters. These conditions are described by the following inequalities:

$$k = 0 : b_2 > 0, \quad a_2 > -\frac{b_2}{n}; \quad (14)$$

$$k = 1 : b_2 > 0 \quad (\text{if } n \geq 3), \quad z_1 > 0,$$

$$d = z_2^2 + z_3 - z_1^2 < 0; \quad (15)$$

$$2 \leq k \leq n - 2 : b_1 > 0, \quad b_2 > 0,$$

$$z_1 > 0, \quad d < 0; \quad (16)$$

$$k = n - 1 : b_1 > 0 \quad (\text{if } n \geq 3),$$

$$z_1 > 0, \quad d < 0; \quad (17)$$

$$k = n : b_1 > 0, \quad a_1 > -\frac{b_1}{n}. \quad (18)$$

The last two inequalities in each line (15)–(17) can be transformed to

$$M_1 : kb_2a_1 + (n - k)b_1a_2 + b_1b_2 > 0, \quad (19)$$

$$M_2 : ka_1 + (n - k)a_2 + (b_1 + b_2) > 0. \quad (20)$$

Inequalities (19), (20) describe two half-planes relative to the coordinates  $(a_1, a_2)$ . Since for the stability of  $\Phi_k$  both of these inequalities must be fulfilled, the values of the parameters  $(a_1, a_2)$  must belong to the region  $M = M_1 \cap M_2$ .

In general,  $M$  is restricted by the lines

$$L_1 : kb_2a_1 + (n - k)b_1a_2 + b_1b_2 = 0, \quad (21)$$

$$L_2 : ka_1 + (n - k)a_2 + (b_1 + b_2) = 0, \quad (22)$$

and contains both stable nodes and stable focuses. A special case corresponds to the situation when  $b_1 = b_2$ . In this case the lines  $L_1, L_2$  are parallel. Taking into account that at least one of the parameters  $b_1$  or  $b_2$  should be positive (and therefore they must both be positive), one can see that the line  $L_2$  locates below the line  $L_1$ . Thus  $M = M_1$ . It is easy to check that for the expression under the root of (10) the inequality

$$z_2^2 + z_3 = \left(\frac{ka_1}{2}\right)^2 + \left(\frac{(n - k)a_2}{2}\right)^2 \geq 0$$

is valid. Therefore  $M$  contains only stable nodes in this case.

Fig. 2 shows some examples of the regions of stability (instability) for different values of parameters.

**Remark 1.** For a fixed value of  $n \geq 3$ , the points  $\Phi_1$  can be the only stable points among other points  $\Phi_k$  ( $k \neq 1$ ). The conditions for that combine inequalities  $b_1 < 0, b_2 > 0, a_2 < -\frac{b_2}{n}$  with conditions (19), (20).

**Remark 2.** The results of this section are valid for any pair of values for which the interaction functions  $f(x)$  and  $g(x)$  are equal to 0 (not obligatory 0 and  $\pi$ ). Moreover, it is sufficient to assume that only one of the functions  $f(x)$  or  $g(x)$  is odd.

### 4. An example

Let us apply the obtained results to an example where the interaction functions  $f(x)$  and  $g(x)$  are represented by the first two terms of the Fourier series expansion of odd functions:

$$\begin{aligned} f(x) &= a(\sin(x) + r \sin(2x)), \\ g(x) &= b(\sin(x) + p \sin(2x)), \end{aligned} \quad (23)$$

where  $a, b, r, p$  are the parameters.

In this case Eqs. (3) take the form:

$$\begin{aligned} \frac{d\varphi_i}{dt} &= - \sum_{j=1}^n a(\sin(\varphi_j) + r \sin(2\varphi_j)) - b(\sin(\varphi_i) + p \sin(2\varphi_i)), \\ & i = 1, \dots, n. \end{aligned} \quad (24)$$

In this example the derivatives of the function  $f(x)$  at the points 0 and  $\pi$  and the derivatives of the function  $g(x)$  at the same points are

$$\begin{aligned} a_1 &= a(2r + 1), & a_2 &= a(2r - 1), \\ b_1 &= b(2p + 1), & b_2 &= b(2p - 1). \end{aligned} \quad (25)$$

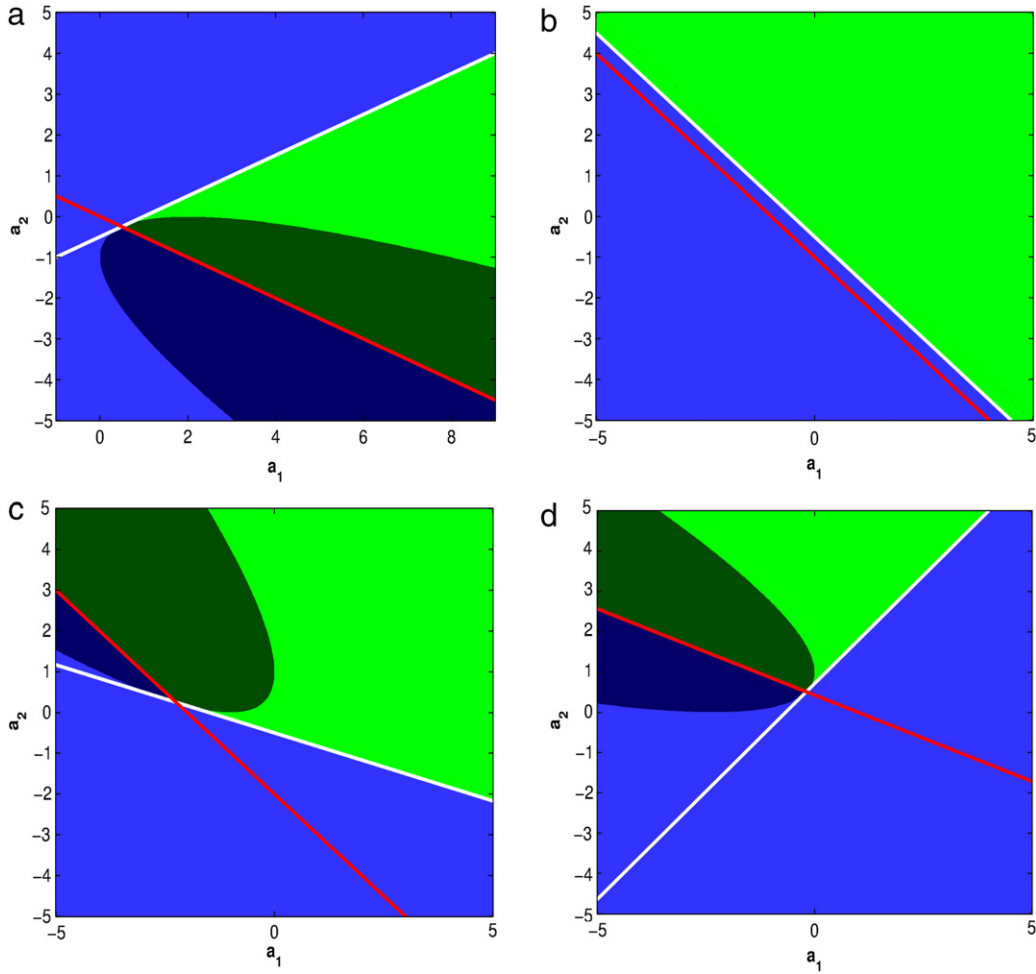


**Fig. 2.** The regions of stability (instability) of the points  $\Phi_k$ . The color notation is: green—stable nodes, dark green—stable foci, blue—unstable nodes, dark blue—unstable foci, white line—the line  $L_1$ , red line—the line  $L_2$ . The values of the parameters: (a)  $n = 3, k = 1, b_1 = -1, b_2 = 1$ ; (b)  $n = 4, k = 2, b_1 = b_2 = 1$ ; (c)  $n = 4, k = 2, b_1 = 3, b_2 = 1$ ; (d)  $n = 10, k = 3, b_1 = 2, b_2 = 5$ .

Using these values in formulas (19), (20) we get

$$M_1 : ab[k(2p - 1)(2r + 1) + (n - k)(2p + 1)(2r - 1) + b^2(4r^2 - 1)] > 0, \quad (26)$$

$$M_2 : a[n(2r - 1) + 2k] + 4pb > 0.$$

Formulas (26) as well as other limitations described by (14)–(18) allow us to formulate stability conditions for the points  $\Phi_k, k = 0, \dots, n$ , for this particular example in terms of the parameters  $a, b, p, r$ . A list of stability conditions is provided in Appendix (Table 1).

**Bifurcations.** The results of the previous section can also be helpful for understanding the mechanism of transitions between different dynamical regimes, in particular, the transitions between stability and instability of the fixed points  $\Phi_k, k = 0, \dots, n$ , under variation of the parameters  $a, b, p, r$ . The peculiarities of the model construction (star-like coupling, equal natural frequencies of oscillators, etc.) imply special invariant structures and bifurcations in the system. The permutation symmetry of POs and oddness of coupling functions are crucial for bifurcation analysis. Due to multiple symmetries, system (24) has two invariant manifolds of a generic type:

(1)  $m$ -dimensional manifolds

$$\mathcal{M}_m = \{(\varphi_1, \dots, \varphi_n) : \varphi_{k_1} = \varphi_{k_2} = \dots = \varphi_{k_{n-m+1}}\}, \\ m = 1, \dots, n,$$

that correspond to  $(n - m + 1)$ -clusters of POs according to their permutation symmetry  $S_n$ , and

(2)  $m$ -dimensional manifolds

$$\mathcal{Q}_m = \{(\varphi_1, \dots, \varphi_n) : \varphi_{k_i} + \varphi_{k_j} = 0, \varphi_{k_i} \in \{0, \pi\}\},$$

$$i = 1, \dots, m, \quad j = 1, \dots, m, \quad j \neq i,$$

$$l = 2m + 1, \dots, n, \quad m = 1, \dots, [n/2],$$

that occur due to odd symmetry of the right hand side of the system.

These invariant manifolds split phase space into invariant regions [21,22].

The points  $\Phi_k$  lose stability via Andronov–Hopf bifurcation when the parameters  $a, b, p, r$  cross the surface:

$$AH(\Phi_k) = \{(a, b, p, r) : 4bp + 2nar + (2k - n)a = 0\},$$

$$k = 1, \dots, n - 1.$$

Another possible bifurcation is the pitchfork bifurcation which appears due to the odd symmetry of the system. The critical surface of the pitchfork bifurcation in parametric space is determined by the following formulas:

$$PF(\Phi_k) = \{(a, b, p, r) : a(n(4pr + 2r - 2p - 1) + 4k(p - r)) + b(4p^2 - 1) = 0\}, \quad k = 1, \dots, n - 1,$$

$$PF(\Phi_n) = \{(a, b, p, r) : b(2p + 1) + na(2r + 1) = 0\},$$

$$PF(\Phi_0) = \{(a, b, p, r) : b(2p - 1) + na(2r - 1) = 0\},$$

which lead to appearance (disappearance) of two new fixed points inside the invariant manifold  $M_m$ .

Other bifurcations of the fixed points  $\Phi_k$  occur under conditions  $b_1 = b(1 - 2p) = 0, b_2 = b(1 + 2p) = 0$ .

- (1)  $p = \pm 1/2$ . In this case several eigenvalues become zero and the degenerate pitchfork bifurcation arises. The critical surface (hyperplane) in parametric space is described by the following formulas:

$$PF_*(\Phi_k) = \{(a, b, p, r) : p = -1/2\}, \quad k = 1, \dots, n,$$

$$PF^*(\Phi_k) = \{(a, b, p, r) : p = 1/2\}, \quad k = 0, \dots, n - 1.$$

The surface formulas do not depend on  $k$ , which means that the bifurcations simultaneously occur for different  $\Phi_k$ . According to system symmetries the pitchfork bifurcations  $PF_*$  and  $PF^*$  occur in  $k - 1$  and  $n - k - 1$  directions simultaneously, giving rise to the appearance of many new fixed points from each  $\Phi_k$ . All new equilibria appear in transversal directions to the invariant manifold and move inside the invariant region under parameter variation.

- (2)  $b = 0$ . In this case the system consists of  $n$  identical equations which include only the coupling from the CO to POs ( $g(x) \equiv 0$ ). It implies that the degenerate ‘switch’ bifurcation appears. The critical surface (hyperplane) in parametric space is described by the following formula:

$$SW(\Phi_k) = \{(a, b, p, r) : b = 0\}, \quad k = 0, \dots, n.$$

The vector field consists of parallel straight lines for the critical parameter value because each equation in (3) has the same right hand side. One eigenvalue of each equilibrium changes its sign to the opposite during the bifurcation. The bifurcation alters the influence of CO  $\rightarrow$  PO from positive to negative and vice versa.

Intersections of codimension-one bifurcation surfaces presented above lead to possible bifurcations of higher codimension-two, three, and four. Note that the bifurcations presented above are not the only bifurcations in system (3) (there can be local bifurcations of a fixed point different from  $\Phi_k$ , fold bifurcations of limit cycles, etc.). Local bifurcations of  $\Phi_k$  can be a part of some global bifurcation, in particular, the heteroclinic bifurcation [22], which is typical for synchronization-clustering-desynchronization transitions in coupled oscillator models. A stable heteroclinic cycle that consists of saddles  $\Phi_k$  connected by their one-dimensional invariant manifolds presents slow switching between different clusters of POs (see Fig. 3(f) for  $n = 2$  and Fig. 11 in [22] for  $n = 3$ ). Some POs can temporarily win the competition for the synchronization. The configuration of the winners changes fast after a long synchronization period.

### 5. Bifurcations in the general case

Considering system (3) with arbitrary odd and periodic coupling functions  $f(x), g(x)$  we find the same bifurcations as in the example described in the previous section. First of all, one can check that system (3) has the same generic invariant manifolds  $\mathcal{M}_m, \mathcal{Q}_m$  which include the points  $\Phi_k$ . Therefore all bifurcations of  $\Phi_k$  occur inside the manifolds or in transversal directions. System (3) has the Andronov–Hopf bifurcation at the points  $\Phi_k$  with conditions described by (22) for  $k = 1, \dots, n - 1$ . Standard pitchfork bifurcations occur when parameters intersect the surfaces described by expressions (21) for  $k = 1, \dots, n - 1$ , and by the formulas  $na_2 + b_2 = 0, na_1 + b_1 = 0$ , for  $k = 1$  and  $k = n$ , respectively.

Let us expand a smooth odd periodic function  $g(x)$  in the Fourier series

$$g(x) = b \sum_{j=1}^{\infty} p_j \sin(jx)$$

with the assumption  $\sum_{j=1}^{\infty} |p_j| < \infty$ . In the example considered above we had  $p_1 = 1, p_2 = p$  and  $p_j = 0, j \geq 3$ . The derivatives of the function  $g(x)$  for  $x = 0$  and  $x = \pi$  are

$$b_1 = b \sum_{j=1}^{\infty} j p_j \quad \text{and} \quad b_2 = b \sum_{j=1}^{\infty} (-1)^{j+1} j p_j.$$

One can check that if either  $b_1 = 0$  or  $b_2 = 0$  system (3) has multiple pitchfork bifurcations  $PF^*$  or  $PF_*$ , respectively.

System (3) also has a degenerative switch bifurcation (SW) for  $b = 0$  that corresponds to switching off the influence from the central oscillator CO  $\rightarrow$  POs. The system does not have any other bifurcations at the points  $\Phi_k$ , but it can have a number of bifurcations of other fixed points, limit and heteroclinic cycles, etc.

### 6. Multistability

*Multistability conditions.* Conditions (14)–(18) guarantee the stability of  $\Phi_k$ . Let us reformulate these conditions to find critical boundaries for the values  $k_1$  and  $k_2$  (under fixed values of other parameters  $a_1, a_2, b_1, b_2$ , and  $n$ ) such that for  $k_1 \leq k \leq k_2$  all fixed points  $\Phi_k$  are stable. Assuming that conditions  $b_1 > 0$  and  $b_2 > 0$  are satisfied we rewrite inequalities (19), (20) and (14)–(18) to obtain multistability conditions. Consider three cases.

- (1)  $b_1 = b_2$ . In this case (14)–(18) also imply  $b_1 = b_2 > 0$ . Using the inequalities  $z_1 > 0, d < 0$  we can estimate the values of  $k$  such that the points  $\Phi_k$  are stable:

$$\text{if } a_1 = a_2, \delta > 0, \quad \text{then } k \in [0, n], \tag{27}$$

$$\text{if } a_1 > a_2, \quad \text{then } k > \kappa_0, \tag{28}$$

$$\text{if } a_1 < a_2, \quad \text{then } k < \kappa_0, \tag{29}$$

where

$$\delta = na_2 + b_2, \quad \kappa_0 = \frac{na_2 + b_2}{a_2 - a_1}.$$

- (2)  $b_1 > b_2$ . In this case system (19), (20) can be rewritten as

$$\text{if } \beta = 0, \delta > 0, \quad \text{then } k \in [0, n], \tag{30}$$

$$\text{if } \beta > 0, \quad \text{then } k > \kappa_1, \tag{31}$$

$$\text{if } \beta < 0, \quad \text{then } k < \kappa_1, \tag{32}$$

where

$$\kappa_1 = \frac{b_1(na_2 + b_2)}{b_1a_2 - b_2a_1}, \quad \beta = b_2a_1 - a_2b_1.$$

- (3)  $b_1 < b_2$ . There are the following six cases of multistability:

$$\text{if } a_1 = a_2, \delta > 0, \quad \text{then } k \in [0, n], \tag{33}$$

$$\text{if } a_1 = a_2, -b_1 < \delta \leq 0, \quad \text{then } k > \kappa_1, \tag{34}$$

$$\text{if } a_1 > a_2, \quad \text{then } k > \max\{\kappa_1, \kappa_2\}, \tag{35}$$

$$\text{if } \beta < 0, \quad \text{then } k < \min\{\kappa_1, \kappa_2\}, \tag{36}$$

$$\text{if } \beta = 0, \delta > 0, \quad \text{then } k < \kappa_2, \tag{37}$$

$$\text{if } a_1 < a_2 < a_1b_2/b_1, \quad \text{then } \kappa_1 < k < \kappa_2 \tag{38}$$

where

$$\kappa_2 = \frac{na_2 + b_1 + b_2}{a_2 - a_1}.$$

Using (27)–(38) we also obtain conditions that guarantee the absence of any stable  $\Phi_k$ :

$$\begin{aligned} \beta = 0, \quad b_1 \geq b_2, \quad \delta \leq 0, \quad \text{or} \\ \beta = 0, \quad b_1 < b_2, \quad \delta \leq -b_1. \end{aligned} \tag{39}$$

Formulas (27)–(38) show that there are regions in parametric space where all fixed points  $\Phi_k, k = 0, \dots, n$ , are stable (maximal multistability). For example, under condition (38) if  $\kappa_1 < 0$  and  $\kappa_2 > n$  then all fixed points are stable.

Thus, for any value of the parameters  $a_1, a_2, b_1, b_2$  except those described by (39) there are the numbers  $k_1 = [k_*(a_1, a_2, b_1, b_2, n) + 1], k_2 = [k_*(a_1, a_2, b_1, b_2, n)]$  ( $k_*$  is the lower boundary of  $k$  in inequalities (27)–(38),  $k^*$  is the upper boundary of  $k$  in these inequalities,  $[x]$  is an integer part of  $x$ ) such that all points  $\Phi_k, k = k_1, \dots, k_2$ , are stable. All points  $\Phi_k$  are stable when both points  $\Phi_0$  and  $\Phi_n$  are stable.

*Regions of multistability.* For a fixed value of  $n$  and other parameters  $(a_1, a_2, b_1, b_2)$ , denote by  $\mathcal{P}_k(a_1, a_2, b_1, b_2, n)$  a nonempty region in parameter space such that the fixed point  $\Phi_k$  is stable. The condition of multistability can be formulated in terms of intersections of regions  $\mathcal{P}_k$ . For example, if intersection of  $\mathcal{P}_1$  and  $\mathcal{P}_2$  is not empty then this intersection is the region of bistability of  $\Phi_1$  and  $\Phi_2$ . In the general case, a region of multistability is determined as an nonempty intersection of  $\mathcal{P}_k$ :

$$\mathcal{P}_J = \bigcap_{k \in J} \mathcal{P}_k,$$

where  $J$  is a set of integer numbers in the range  $\{0, 1, \dots, n\}$ .

We illustrate that in system (24) there is a set of monotonically increasing regions  $\mathcal{P}_0 \subset \mathcal{P}_1 \subset \dots \subset \mathcal{P}_n$ . This monotonic sequence of regions enables us to characterize multistability regions  $\mathcal{P}_J$ .

Fig. 4 shows two cases of multistability in system (24) with one CO and fifteen POs ( $n = 15$ ): (a) the parameter  $r$  varies and all other parameters are fixed ( $a = -0.06, b = 1, p = 0.6$ ); (b) the parameter  $p$  varies and all other parameters are fixed ( $a = 0.5, b = 1, r = 0.35$ ). The horizontal lines in Fig. 4(a) correspond to three values of the parameter  $r$ : ( $r = 0.54, r = 0.62, r = 0.7$ ). Considering conditions (27)–(38) for the chosen parameter values we can find that  $b_1 = 2.2 > b_2 = 0.2$  in all cases and  $\beta = -0.0144 < 0$  in the first case only; in two other cases  $\beta$  is positive ( $\beta = 0.0048, \beta = 0.024$ ). Therefore, conditions (31) and (32) are satisfied. Thus,  $r = 0.54$  implies multistability for any  $k \in J = \{0, 1, \dots, 15\}$  ( $\kappa_1 \approx 19.56 > 15$ ),  $r = 0.62$  implies multistability for any  $k \in J = \{8, 9, \dots, 15\}$  ( $\kappa_1 \approx 7.33 < 8$ ),  $r = 0.7$  implies the stability of  $\Phi_k$  only (no multistability) for  $k = 15$  ( $\kappa_1 \approx 14.67 < 15$ ). In Fig. 4(a) regions  $\mathcal{P}_k$  are shown by vertical blue bars  $[0, \bar{r}(k)]$ , where  $\bar{r}(k) = (0.144k - 2.42)/(0.24k - 3.96)$ . Similarly, Fig. 4(b) shows multistability regions  $\mathcal{P}_k$  (blue vertical bars) under the variation of the parameter  $p$ .

Fig. 5 shows the bifurcation diagram of system (24) under the variation of two parameters  $p$  and  $r$ . Pitchfork bifurcation lines  $PF(\Phi_k), k = 0, 1, \dots, 15$ , are shown by variable colors (from blue to red) and some of these curves are labeled by  $k = 0, k = 14, k = 15$ . The blue curve shows the common degenerate bifurcation  $PF^*$ . Regions of multistability are yellow, the region of instability is dark cyan and the region with one stable fixed point is filled by light cyan. The regions  $\mathcal{P}_k, k = 0, \dots, 13$ , are bounded at the left side by the vertical green line of the degenerate pitchfork bifurcation and at the top by  $PF(\Phi_k)$  (variable color). The regions  $\mathcal{P}_{14}$  and  $\mathcal{P}_{15}$  are bounded at the left side only by the  $PF(\Phi_{14})$  and  $PF(\Phi_{15})$  bifurcation lines, respectively. Bistability occurs in the region  $\mathcal{P}_{14}$  and multistability of all  $\Phi_k$  occurs in the region  $\mathcal{P}_0$  because  $\mathcal{P}_{15} \supset \mathcal{P}_{14} \supset \dots \supset \mathcal{P}_1 \supset \mathcal{P}_0$ .

*Coexistence of  $\Phi_k$  and other attractors.* Two possible cases occur in system (3) concerning  $\Phi_k$  equilibria:

- (1) there exist only fixed points  $\Phi_k$ ;
- (2) these points coexist with other fixed points.

The first case mostly happens when the coupling functions  $f(x), g(x)$  intersect the horizontal coordinate line at the points  $0, \pi$  only (except a few special cases, like  $g(x) = nf(x)$ , for example). The permutation symmetry  $S_n$  implies multistability of  $C_n^k$  points of the same type  $\Phi_k$  with all possible sequences of 0 and  $\pi$  if one of these points is stable. Using time reverse symmetry characterized by the transformation

$$\gamma : (\varphi_1, \dots, \varphi_n, t) \mapsto (-\varphi_1, \dots, -\varphi_n, -t)$$

and conditions (14)–(18), one can find regions where the points  $\Phi_k$  are sources (changing the proper signs in the inequalities). Then conditions when any  $\Phi_k$  is a saddle can be written as a corollary. Heteroclinic connections appear when the system has only saddle equilibria  $\Phi_k$ . It is shown in [22] that such heteroclinic connections can be stable themselves and they can lead to ABC-like chaotic flows.

The case of coexistence of  $\Phi_k$  with other fixed points mostly occurs when connection functions have more than two intersections with the horizontal coordinate line. Multistability of two fixed points of different types is possible as far as coexistence of  $\Phi_k$  with attractors of other types.

The multistability already occurs in the simplest nontrivial case CO + 2POs. A few such cases are shown in Fig. 3. One can see the coexistence of different stable  $\Phi_i, i = 0, 1, 2$ , configurations in the cases (a)–(c), the coexistence of the stable equilibria  $\Phi_1$  with a stable heteroclinic cycle (d), and the coexistence of the stable equilibrium  $\Phi_2$  with other stable equilibria different from any  $\Phi_i$  (e). In the last case (f) shown in the figure all equilibria of the system are unstable (sources and saddles) but two of them form a stable structure (a heteroclinic cycle).

As far as the system is multistable for most values of the parameters, possible attractors split the whole phase space into their own basins of attraction. Even in the simplest case when the system has only one type of attractors  $\Phi_{k_0}, k_0 \neq n$  (no stable limit or heteroclinic cycles, etc.) phase space is split into  $C_n^k$  equivalent regions of attraction corresponding to the symmetry. The attraction regions of different regimes  $\Phi_k$  change with parameter variation (Fig. 3). Therefore we can partially control the size of attraction basins  $m(\Omega_k)$  of different stable points we are interested in. The problem of finding parametric regions where the points  $\Phi_k$  are the only attractors of system (24) (important for biological applications) has been studied in [22].

### 7. A system with local connections between peripheral oscillators

Suppose that POs are coupled by local connections with an architecture shown in Fig. 1(b)–(e). In this case the equations for system dynamics are

$$\frac{d\theta_0}{dt} = \omega_0 + \sum_{i=1}^n f(\theta_i - \theta_0), \tag{40}$$

$$\frac{d\theta_i}{dt} = \omega_i + g(\theta_0 - \theta_i) + \sum_{k \in N_i} h(\theta_k - \theta_i), \quad i = 1, \dots, n, \tag{41}$$

where  $h(x)$  is the interaction function for local coupling (odd, continuous,  $2\pi$ -periodic) and  $N_i$  are the neighbors of the  $i$ th PO. Below we assume that conditions

$$f'(0) = a_1, \quad g'(0) = b_1, \quad h'(0) = c > 0, \tag{42}$$

$$\omega_i = \omega, \quad i = 0, \dots, n$$

are fulfilled.

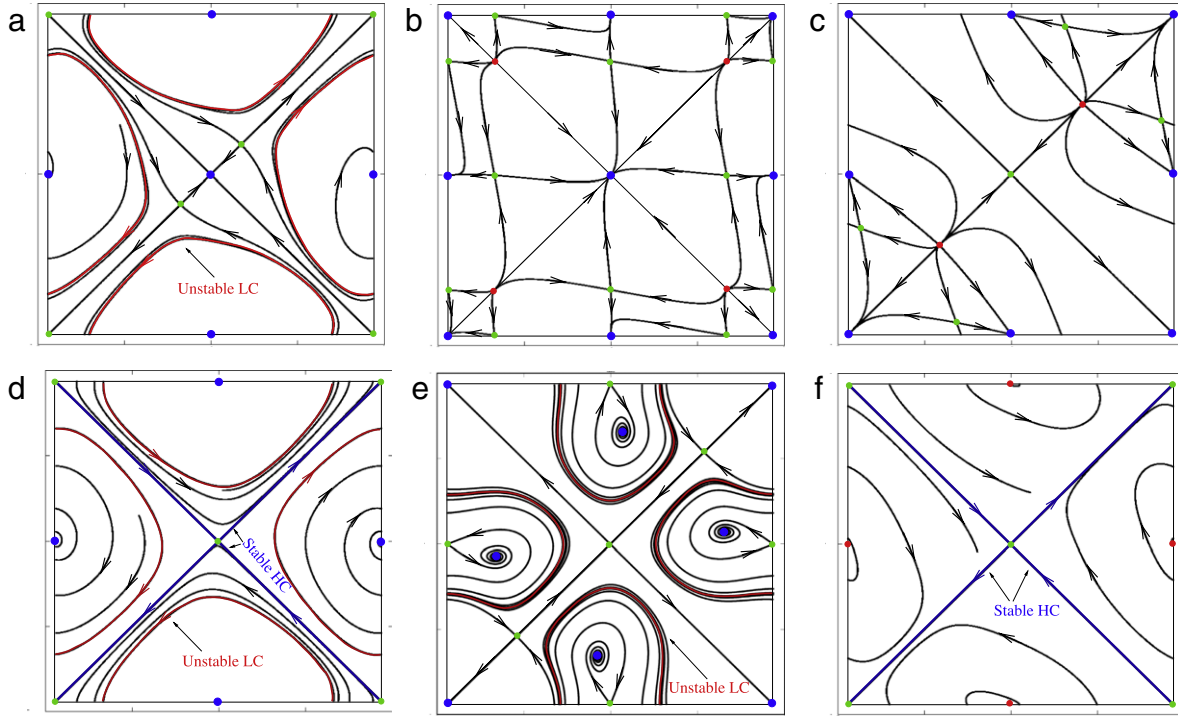


**Fig. 3.** Phase portraits for  $\varphi_1, \varphi_2 \in [0, 2\pi]$  show multistability in (24) for CO+2POs. Attractors, repellers, and saddles are indicated by blue, red, and green colors, respectively. The system demonstrates coexistence of the following attractors: (a)  $\Phi_0$  and  $\Phi_1$ ; (b)  $\Phi_0, \Phi_1$  and  $\Phi_2$ ; (c)  $\Phi_1$  and  $\Phi_2$ ; (d)  $\Phi_1$  and the heteroclinic cycle  $HC(\Phi_0, \Phi_2)$ ; (e)  $\Phi_2$  and four  $D_2$ -symmetric points that belong to invariant regions bounded by invariant lines. The system does not have any stable equilibria in the case (f) but it has a stable heteroclinic cycle formed by two saddles  $\Phi_0, \Phi_2$  and their 1D invariant manifolds. The corresponding values of the system parameters ( $a, b, p, r$ ) are: (a) (1, -1, 0, 0.1); (b) (0.2, -1, -0.8, -0.8); (c) (-0.45, 1, -0.49, 0, 49); (d) (1, -1, 0, 0, 3); (e) (-0, 7, 1, -0.8, -0.4) (f) (0.7, -1, 0.4, 0.4). (For interpretation of the references to colour in this figure legend, the reader is referred to the web version of this article.)

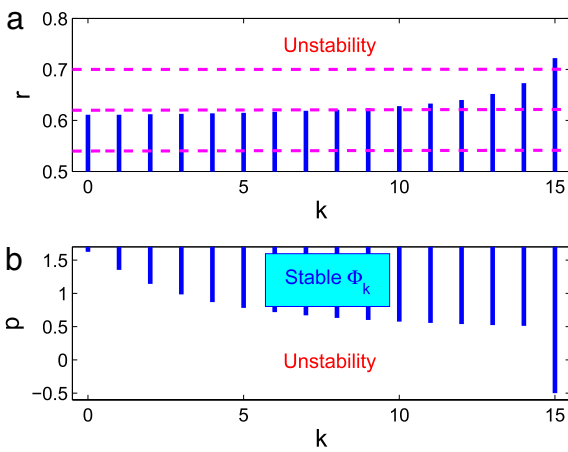


**Fig. 4.** Multistability examples for 15 peripheral oscillators in (24). The horizontal axis  $k$  indicates the number of PO (discrete values for  $k = 0, \dots, 15$ ), the vertical axis shows: (a) the values of the parameter  $r$  for the fixed parameter values  $a = -0.06, b = 1, p = 0.6$ ; (b) the values of the parameter  $p$  for fixed parameter values  $a = 0.5, b = 1, r = 0.35$ . Vertical (blue) lines show the values of the parameters  $r$  and  $p$  where the points  $\Phi_k$  are stable. The horizontal dashed lines indicate fixed values of the parameter  $r = 0.54, r = 0.62$ , and  $r = 0.7$  in (a). Multistability of 16 and 8 points occur in the first two cases, only one point  $\Phi_{15}$  is stable in the last case. (For interpretation of the references to colour in this figure legend, the reader is referred to the web version of this article.)

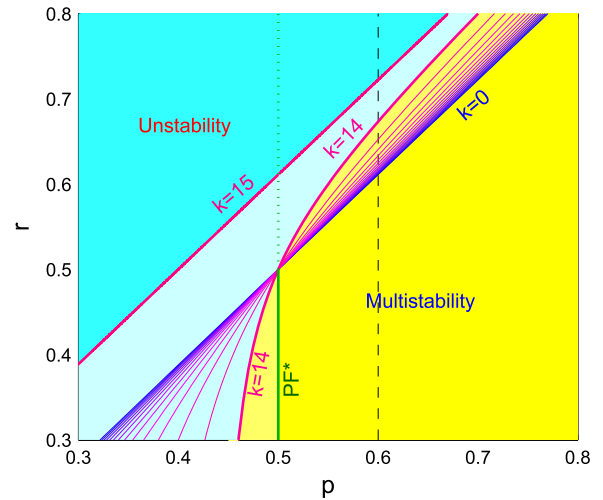


**Fig. 5.** Bifurcation diagram on the  $(p, r)$ -plane for  $n = 15, a = -0.06, b = 1$ . The stability regions for different points  $\Phi_k, k = 0, \dots, 13$ , are bounded at the left by the pitchfork bifurcation lines  $PF(\Phi_k)$  with different numbers  $k$  (shown in the diagram) and the common pitchfork line  $PF^*$  ( $r \leq 0.5$ ). In the cases  $k = 14$  and  $k = 15$  (full synchronization) the stability regions are bounded only by  $PF(\Phi_{14})$  and  $PF(\Phi_{15})$  lines, respectively. The hierarchy  $\mathcal{P}_{k_1} \subset \mathcal{P}_{k_2}$  for  $k_1 < k_2$  takes place implying multistability of  $\Phi_k$  (yellow). (For interpretation of the references to colour in this figure legend, the reader is referred to the web version of this article.)

Eqs. (3) for phase differences will now take the form

$$\frac{d\varphi_i}{dt} = - \sum_{j=1}^n f(\varphi_j) - g(\varphi_i) - \sum_{k \in N_i} h(\varphi_i - \varphi_k), \quad i = 1, \dots, n. \quad (43)$$

If the CO were switched off, it is easy to see that the regime when all POs work in-phase would be asymptotically stable due to synchronizing local connections. The introduction of the CO with

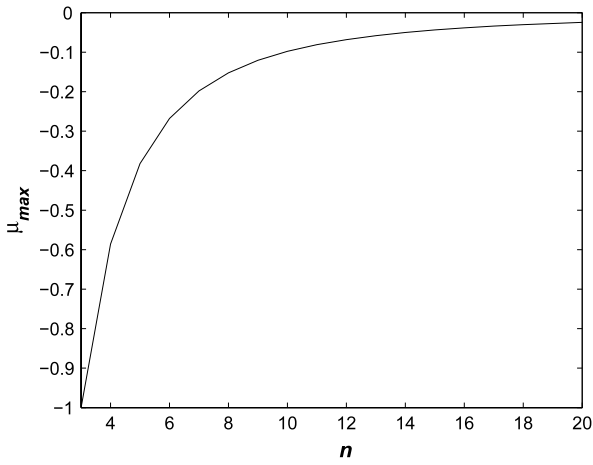


Fig. 6. Maximal roots of the equation  $\det S_{n-1}(\mu) = 0$ .

repulsive influence on POs may break the stability of the point  $\Phi_n = (0, \dots, 0)$ .

Let us compute the eigenvalues of system (43) at the point  $\Phi_n$ . First consider the one-dimensional case shown in Fig. 1(b). The eigenvalues are determined from the equation

$$(b_1 + na_1 + \lambda) \det E_{n-1}(\lambda) = 0, \tag{44}$$

where  $E_{n-1}(\lambda)$  is the  $(n - 1) \times (n - 1)$ -dimensional matrix (see Box 1).

Thus, one eigenvalue is

$$\lambda_1 = -b_1 - na_1 \tag{45}$$

and other eigenvalues are the roots of the equation  $\det E_{n-1}(\lambda) = 0$ . These roots can be represented as

$$\lambda = -b_1 + c\mu, \tag{46}$$

where  $\mu$  are the roots of the equation

$$\det S_{n-1}(\mu) = \det \begin{pmatrix} 2 + \mu & -1 & 0 & \dots & 0 & 0 \\ -1 & 2 + \mu & -1 & \dots & 0 & 0 \\ 0 & -1 & 2 + \mu & \dots & 0 & 0 \\ \dots & \dots & \dots & \dots & \dots & \dots \\ 0 & 0 & 0 & \dots & 2 + \mu & -1 \\ 0 & 0 & 0 & \dots & -1 & 2 + \mu \end{pmatrix} = 0. \tag{47}$$

Maximal values of the roots of the equation  $\det S_{n-1}(\mu) = 0$  (as a function of  $n$ ) are shown in Fig. 6. Note that the curve locates below zero and rapidly approaches zero when  $n$  increases.

Suppose that the interaction between the CO and POs is one-directional (from POs to the CO only) and synchronizing, that is  $b_1 = 0$  and  $a_1 > 0$ . Then from (45)–(47) and Fig. 6 it follows that all eigenvalues are negative, thus the point  $\Phi_n$  is asymptotically stable. This stability is evidently kept if the interaction between the CO and POs is two-directional and synchronizing,  $a_1 > 0$  and  $b_1 > 0$ . The situation is quite different if the influence of the CO on POs is desynchronizing, that is if  $a_1 > 0$  and  $b_1 < 0$ . The first eigenvalue (45) can be made negative if  $n$  is large enough, but (46) and Fig. 6 show that for large enough  $n$  the largest eigenvalue becomes positive even for a small absolute value of  $b_1$ , thus if  $n$  increases the point  $\Phi_n$  relatively quickly becomes unstable.

Fig. 7 allows one to compare the conditions of stability for different architectures shown in Fig. 1(b)–(e). Computations confirm the intuitive feeling that the POs arrangement on the circle and on the torus have higher resistance to the desynchronizing influence of the CO than the arrangement on the line or on the plane grid. The unexpected result of computations is that the graphs of maximal eigenvalues as functions of  $n$  turned to be identical for POs on the line and on the square plane grid. Also they are identical for the ring and for the torus.

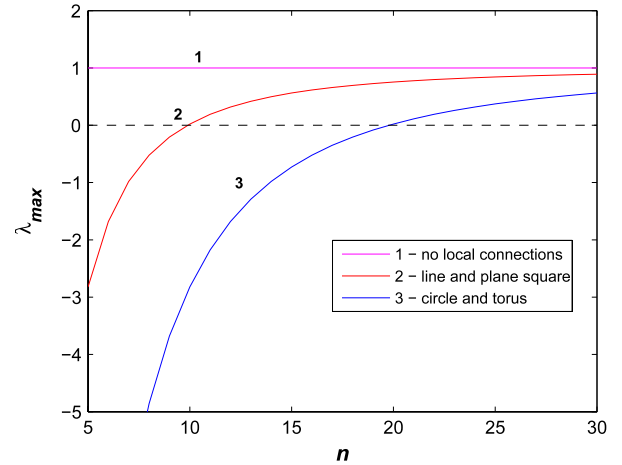


Fig. 7. Maximal eigenvalues for different architectures of connections: 1—no local connections between POs (magenta straight line); 2—coupling on the line or on the square plane grid (red curve); 3—coupling on the circle or on the torus (blue curve). The parameters are  $a_1 = 10$ ,  $b_1 = -1$ ,  $c = 10$ . (For interpretation of the references to colour in this figure legend, the reader is referred to the web version of this article.)

**Remark 3.** The identical behavior of the graphs in Fig. 7 in 1D and 2D cases shows that the conditions for synchronization of the system can be more correctly described in terms of the linear size of the system instead of the number of oscillators in it.

**Remark 4.** The results of this section are valid for any fixed point with identical coordinates (not obligatory  $\Phi_n$ ) of system (43).

It is interesting to compare system (40)–(41) with local connections and the system with global connections between POs (Fig. 1(f)). In this case the eigenvalues for the point  $\Phi_n$  are

$$\lambda_1 = -na_1 - b_1 - c \quad \text{and} \quad \lambda_{2,\dots,n} = -b_1 - (n + 1)c.$$

Thus the conditions of asymptotic stability for the point  $\Phi_n$  are

$$c > -na_1 - b_1 \quad \text{and} \quad c > -\frac{b_1}{n + 1}.$$

If  $a_1 > 0$ ,  $b_1 < 0$ ,  $c > 0$ , both inequalities are fulfilled for a large enough value of  $n$ .

### 8. Discussion

In this paper we investigated the stability of some fixed points in a system of phase oscillators with a central unit. Two types of network connection architectures have been considered: the networks with and without local connections between POs. In the case of star-coupled networks we obtained analytical description of the parameter regions where POs compete for the synchronization with the CO and only a given number of POs can win this competition. Thus we obtain a generalized version of the winner-take-all procedure when the number of winners is controlled by the parameters of the system.

The results were applied to an important class of interaction functions (23) allowing us to describe the bifurcations that lead to the transitions between stability and instability of the fixed points  $\Phi_k$ ,  $k = 0, \dots, n$ , under variation of the parameters. Moreover, it was possible to describe the most important bifurcations that can appear in the general case of odd interaction functions. Since stable points  $\Phi_k$  can coexist for different values of  $k$ , we derived

$$E_{n-1} = \begin{pmatrix} b_1 + 2c + \lambda & -c & 0 & \cdots & 0 & 0 \\ -c & b_1 + 2c + \lambda & -c & \cdots & 0 & 0 \\ 0 & -c & b_1 + 2c + \lambda & \cdots & 0 & 0 \\ \cdots & \cdots & \cdots & \cdots & \cdots & \cdots \\ 0 & 0 & 0 & \cdots & b_1 + 2c + \lambda & -c \\ 0 & 0 & 0 & \cdots & -c & b_1 + 2c + \lambda \end{pmatrix}.$$

Box I.

conditions and developed a procedure that guarantees that the system has a particular type of multistability under a proper selection of parameter values.

The results of Sections 3–6 can be considered as a generalization of our study of small systems of phase oscillators [22]. Previous results were obtained for the networks with two or three POs and a special type of interaction functions (23). Now we have canceled any restrictions on the size of the network and used interaction functions of a very general form.

The only significant restriction is the assumption that the interaction functions  $f(x)$ , (or  $g(x)$ ) and  $h(x)$  are odd. This assumption is used due to a technical reason: we use this assumption to derive Eq. (3) from Eqs. (1) to (2) (similarly, Eq. (43) from Eqs. (40) to (41)). In fact this assumption can be relaxed by using the derivatives of the function  $f_1(x) = f(-x)$  instead of the derivatives of the odd function  $f(x)$  (similarly, using the derivatives of  $h_1(x) = h(-x)$  instead of the derivatives of the odd function  $h(x)$ ). However, this assumption is essential for the bifurcation analysis in Sections 4–6 where we consider interaction functions of a particular type. For example, the pitchfork bifurcation requires that the interaction function is odd.

Phase oscillator systems with a CO and local connections between POs avoided attention of researchers somehow. Still their dynamical behavior is interesting and to some extent unpredictable. As we show, in contrast to the systems with global synchronizing connections between POs whose synchronization is very stable, the synchronization in large systems with local connections can be disrupted even by a weak desynchronizing influence of the CO. The architectures on the circle or on the torus are a bit more stable than the architectures on the line or on the plane grid but their advantage rapidly disappears when the linear size of the network increases.

Note that the point  $\Phi_n$  can be a stable point of a system without local connections and desynchronizing influence of the CO for  $n = 1$  only. If local connections are present, they turn independent POs into an ensemble of coherent POs that interacts with the CO as if it were a single oscillator. But this ensemble is stable if only its size is small enough. Otherwise it cannot resist the desynchronizing influence of the CO and its coherence is destroyed.

Our interest in system (1)–(2) and its stable states is related to the application of this system (or its generalization) as a model of selective attention [23–28]. The systems with relaxation oscillators and a central inhibitory neuron, the systems with Hodgkin–Huxley type neurons and star-like connections, as well as phase oscillator systems of other architectures were used as attention models [29–33]. Selective attention is a built-in mechanism of perception that allows the animals to extract from the large amount of simultaneously obtained information a smaller part (which is usually of significant importance) that should be processed in more detail. There is a hypothesis that the attention system has hierarchical structure with a special controlling subsystem (called the central executive) at its top that controls the formation of the focus of attention [34–36]. Recent experiments have shown that the interaction of the central executive with neural assemblies representing visual objects may be realized by synchronizing their activities at gamma band frequency [37]. This evidence is in line with the gen-

eral concept of the temporal correlation theory which states that a single object is represented in the cortex by synchronized activity of a neural population specific for this object [38].

According to the model assumptions, the CO represents the central executive of the attention system (assumed to be a distributed network in the prefrontal cortex) and POs represent neural assemblies in the association cortex whose activity is elicited by external objects that are simultaneously present at the input of the visual system. In terms of the model, an object is included in the focus of attention if the POs that code this object work synchronously (in-phase) with the CO. Other POs (representing distracting objects) should be out of phase relative to the CO. Therefore the regime of in-phase/anti-phase relations between the CO and POs can be interpreted as attention focusing on a single object ( $k = 1$ ) or on several objects ( $k > 1$ ). The latter case can be interpreted as divided attention. Note that the model LEGION of consecutive selection of objects [39] built of relaxation oscillators also demonstrates phase shifts in the activity of oscillators representing different objects but this model does not allow one to control the number of objects in the focus of attention.

In the simplest case it is assumed that each object is coded by a single PO. This case is modeled by a star-coupled network. The results obtained in Sections 3–6 provide a general view on the parameter regions of the model that allow the objects to compete for attention attraction. In a more realistic situation an object is represented by an assembly of coherent POs. In this case the question arises whether this coherence is stable under the influence of the CO. This question has been studied in Section 7. The results show that without massive usage of global connections one should be careful in using desynchronizing connections from the CO to POs in order to organize the competition between the assemblies of locally connected POs for the synchronization with the CO. This destroys the coherence in the assembly if its size is large enough. This may probably be the reason for the fact that visual attention is usually spread on a rather small portion of the visual field at each moment of time while attention to a large object is implemented through saccades.

## Acknowledgment

O.B. was supported by the Centre for Robotics and Neural Systems, Faculty of Science and Technology, University of Plymouth.

## Appendix

Expression (25) for the derivatives of functions (23) provides the possibility to explicitly find the regions of the parameters  $a$ ,  $b$ ,  $r$ ,  $p$  where inequalities (14)–(18) are fulfilled. The results of computations of these regions are summarized in Table 1 which provides an explicit description of the interaction functions that guarantee a particular number of asymptotically stable points  $\Phi_k$ . In this table we consider only the values of  $n$  greater than 3 since similar results for the case  $n = 2$  can be easily extracted from our previous publication [22]. For  $k$  ( $1 \leq k \leq n - 1$ ) the results are obtained by solving inequalities (26) together with one or both inequalities  $b_1 = b(2p + 1) > 0$ ,  $b_2 = b(2p - 1) > 0$ .

**Table 1**  
Conditions for asymptotic stability,  $n \geq 3$ .

$p = r$	$k = 0$	$b > 0$	$a > -\frac{b}{n}$ for $r > \frac{1}{2}$
		$b < 0$	$a < -\frac{b}{n}$ for $r < \frac{1}{2}$
	$k = 1$	$b > 0$	$a > -\frac{b}{n}$ for $r > \frac{1}{2}$
		$b < 0$	$a > -\frac{2br}{n(r-q)}$ for $q < r < \frac{1}{2}$
			$-\frac{b}{n} < a < -\frac{2br}{n(r-q)}$ for $-\frac{1}{2} < r \leq -q$
		$a < -\frac{b}{n}$ for $r < -\frac{1}{2}$ where $q = \frac{n-2}{2n}$	
	$2 \leq k \leq n-2$	$b > 0$	$a > -\frac{b}{n}$ for $r > \frac{1}{2}$
		$b < 0$	$a < -\frac{b}{n}$ for $r < -\frac{1}{2}$
	$k = n-1$	$b > 0$	$a > -\frac{b}{n}$ for $r > \frac{1}{2}$
			$-\frac{2br}{n(r+q)} < a < -\frac{b}{n}$ for $q < r < \frac{1}{2}$
		$b < 0$	$a < -\frac{b}{n}$ for $r < -\frac{1}{2}$
	$k = n$	$b > 0$	$a > -\frac{b}{n}$ for $r > -\frac{1}{2}$
$b < 0$		$a < -\frac{b}{n}$ for $r < -\frac{1}{2}$	
$r \neq 0, p = 0$	$k = 0$	$b > 0$	$a > \frac{b}{n(2r-1)}$ for $r > \frac{1}{2}$
		$b < 0$	$a < \frac{b}{n(2r-1)}$ for $r < \frac{1}{2}$
	$k = 1$	$b < 0$	$a > \frac{b}{2r(n-2)-n}$ for $\frac{1}{2} - \frac{1}{n} < r < \frac{n}{2(n-2)}$
	$k = n-1$	$b > 0$	$a < \frac{b}{2r(n-2)+n}$ for $-\frac{n}{2(n-2)} < r < -\frac{1}{2} + \frac{1}{n}$
$k = n$	$b > 0$	$a > -\frac{b}{n(2r+1)}$ for $r > -\frac{1}{2}$	
		$a < -\frac{b}{n(2r+1)}$ for $r < -\frac{1}{2}$	
$r = 0, p \neq 0$	$k = 0$	$b > 0$	$a < \frac{b(2p-1)}{n}$ for $p > \frac{1}{2}$
		$b < 0$	$a < \frac{b(2p-1)}{n}$ for $p < \frac{1}{2}$
		$b > 0$	$a < \frac{b(4p^2-1)}{2p(n-2)+n}$ for $p > \frac{1}{2}$
	$k = 1$	$b < 0$	$\frac{b(4p^2-1)}{2p(n-2)+n} < a < \frac{4bp}{n-2}$ for $-u < p \leq p_1$
			$a < \frac{4bp}{n-2}$ for $p_2 < p \leq -u$
	$2 \leq k < \frac{n}{2}$	$b > 0$	$a < \frac{b(4p^2-1)}{2p(n-2k)+n}$ for $p > \frac{1}{2}$
			$\frac{b(4p^2-1)}{2p(n-2k)+n} < a < \frac{4bp}{n-2k}$ for $-s < p < -\frac{1}{2}$
		$b < 0$	$a < \frac{4bp}{n-2k}$ for $p_2 < p \leq -s$
			$a < \frac{b(4p^2-1)}{2p(n-2k)+n}$ for $p \leq p_2$ where $s = \frac{n}{2(n-2k)}, p_{1,2} = -s \pm \sqrt{s^2 - \frac{1}{4}}$
	$k = \frac{n}{2}$	$b > 0$	$a < \frac{b(4p^2-1)}{n}$ for $p > \frac{1}{2}$
		$b < 0$	$a > \frac{b(4p^2-1)}{n}$ for $p < -\frac{1}{2}$
	$\frac{n}{2} < k \leq n-2$	$b > 0$	$a > \frac{b(4p^2-1)}{2p(n-2k)+n}$ for $p \geq p_1$
			$a > \frac{4bp}{n-2k}$ for $-s \leq p < p_1$
		$b < 0$	$\frac{4bp}{n-2k} < a < \frac{b(4p^2-1)}{2p(n-2k)+n}$ for $\frac{1}{2} < p \leq -s$
	$k = n-1$	$b > 0$	$a > \frac{b(4p^2-1)}{2p(n-2k)-n}$ for $p \geq p_1$
			$a > \frac{4bp}{n-2k}$ for $s \leq p < p_1$
		$b < 0$	$-\frac{4bp}{n-2k} < a < -\frac{b(4p^2-1)}{2p(n-2k)-n}$ for $p_2 \leq p < s$
	$k = n$	$b > 0$	$a > -\frac{b(4p^2-1)}{2p(n-2k)-n}$ for $p < -\frac{1}{2}$
		$b < 0$	$a > -\frac{b(2p+1)}{n}$ for $p > -\frac{1}{2}$
	$b < 0$	$a > -\frac{b(2p+1)}{n}$ for $p < -\frac{1}{2}$	

## References

- [1] Y. Kuramoto, *Chemical Oscillations, Waves and Turbulence*, Springer-Verlag, Berlin, 1984.
- [2] J.A. Acebron, L.L. Bonilla, C.J. Perez Vicente, R. Spigler, The Kuramoto model: a simple paradigm for synchronization phenomena, *Rev. Modern Phys.* 77 (2005) 137–185.
- [3] A. Arenas, A. Diaz-Guilera, J. Kurths, Y. Moreno, C. Zhou, Synchronization in complex networks, *Phys. Rep.* 469 (2008) 93–153.
- [4] A. Pikovsky, M. Rosenblum, J. Kurths, *Synchronization, A Universal Concept in Nonlinear Sciences*, Cambridge University Press, Cambridge, 2001.
- [5] S.H. Strogatz, From Kuramoto to Crawford: exploring the onset of synchronization in populations of coupled oscillators, *Physica D* 143 (2000) 1–20.
- [6] A. Damasio, The brain binds entities and events by multiregional activation from convergent zones, *Neural Comput.* 1 (1989) 123–132.
- [7] C. Zhou, L. Zemanova, G. Zamora, C.C. Hilgetag, J. Kurths, Hierarchical organization unveiled by functional connectivity in complex brain networks, *Phys. Rev. Lett.* 97 (2006) 238103.
- [8] D. Golomb, D. Hansel, B. Shraiman, H. Sompolinsky, Clustering in globally coupled phase oscillators, *Phys. Rev. A* 45 (1992) 3516–3530.
- [9] D. Huang, G. Pipa, Achieving synchronization of networks by an auxiliary hub, *EPL* 77 (2007) 50010.
- [10] Y. Kazanovich, R. Borisyuk, Synchronization in oscillator systems with a central element and phase shifts, *Progr. Theor. Phys.* 110 (2003) 1047–1058.
- [11] F. Sorrentino, M. di Bernardo, G. Huerta Cuellar, S. Boccaletti, Synchronization in weighted scale free networks with degree–degree correlation, *Physica D* 224 (2006) 123–129.
- [12] K.Y. Tsang, R.E. Mirollo, S.H. Strogatz, K. Wiesenfeld, Dynamics of a globally coupled oscillator array, *Physica D* 48 (1991) 102–122.
- [13] J.W. Swift, S.H. Strogatz, K. Wiesenfeld, Averaging of globally coupled oscillators, *Physica D* 55 (1992) 239–250.
- [14] S. Watanabe, S.H. Strogatz, Constants of motion for superconducting Josephson arrays, *Physica D* 74 (1994) 197–253.
- [15] A. Marvel, R.E. Mirollo, S.H. Strogatz, Identical phase oscillators with global sinusoidal coupling evolve by Möbius group action, *Chaos* 19 (2009) 043104.
- [16] I. Belykh, M. Hasler, Synchronization and graph topology, *Int. J. Bifurcation Chaos* 15 (2005) 3423–3433.
- [17] U. Rutishauser, R. Douglas, State-dependent computational using coupled recurrent networks, *Progr. Theoret. Phys.* 21 (2009) 478–509.
- [18] I. Omelchenko, Yu. Maistrenko, E. Mosekilde, Synchronization in ensembles of coupled maps with a major element, *Discrete Dyn. Nat. Soc.* (2005) 239–255.
- [19] M. Frasca, A. Bergner, J. Kurths, L. Fortuna, Bifurcations in star-like network of Stuart–Landau oscillators, *Int. J. Bifurcation Chaos* 22 (2012) 1250173.
- [20] H. Hong, S.H. Strogatz, Conformists and contrarians in a Kuramoto model with identical natural frequencies, *Phys. Rev. E* 84 (2011) 046202.
- [21] P. Ashwin, J.W. Swift, The dynamics of  $n$  weakly coupled identical oscillators, *J. Nonlinear Sci.* 2 (1992) 69–108.
- [22] O. Burylko, Y. Kazanovich, R. Borisyuk, Bifurcations in phase oscillator networks with a central element, *Physica D* 241 (2012) 1072–1089.
- [23] V.I. Kryukov, An attention model based on the principle of dominance, in: A.V. Holden, V.I. Kryukov (Eds.), *Neurocomputers and Attention I. Neurobiology, Synchronization and Chaos*, Manchester University Press, Manchester, 1991, pp. 319–352.
- [24] V.I. Kryukov, The role of the hippocampus in long-term memory: is it memory store or comparator? *J. Integr. Neurosci.* 7 (2008) 117–184.
- [25] Y. Kazanovich, R. Borisyuk, Dynamics of neural networks with a central element, *Neural Netw.* 12 (1999) 441–454.
- [26] R. Borisyuk, Y. Kazanovich, Oscillatory neural network model of attention focus formation and control, *BioSystems* 71 (2003) 29–38.
- [27] R. Borisyuk, Y. Kazanovich, Oscillatory model of attention-guided object selection and novelty detection, *Neural Netw.* 17 (2004) 899–915.
- [28] R. Borisyuk, Y. Kazanovich, Oscillations and waves in the models of interactive neural populations, *BioSystems* 86 (2006) 53–62.
- [29] Z. Wu, A. Guo, Selective visual attention in a neurocomputational model of phase oscillators, *Biol. Cybern.* 80 (1999) 2005–2014.
- [30] S. Corchs, G. Deco, *Neurocomputing* 38 (2001) 1151–1160.
- [31] M.G. Quiles, D.L. Wang, L. Zhao, R.A.F. Romero, D. Huang, Selecting salient objects in real scenes: an oscillatory correlation model, *Neural Netw.* 24 (2011) 54–64.
- [32] D. Chick, R. Borisyuk, Y. Kazanovich, Selective attention model with spiking elements, *Neural Netw.* 22 (2009) 890–900.
- [33] J. Qu, J. R. Wang, Y. Du, An improved selective attention model considering orientation preferences, *Neural Comput. Appl.* 22 (2013) 303–311.
- [34] A. Baddeley, Exploring the central executive, *Q. J. Exp. Psychol.* 49A (1996) 5–28.
- [35] A. Baddeley, Fractionating the central executive, in: D. Stuss, R.T. Knight (Eds.), *Principles of Frontal Lobe Function*, Oxford University Press, New York, 2002, pp. 246–260.
- [36] N. Cowan, Evolving conceptions of memory storage, selective attention and their mutual constraints within the human information processing system, *Psychol. Bull.* 104 (1988) 163–191.
- [37] G.G. Gregoriou, S.J. Gotts, H. Zhou, R. Desimone, High-frequency, long-range coupling between prefrontal and visual cortex during attention, *Science* 324 (2009) 1207–1210.
- [38] W. Singer, C.M. Gray, Visual feature integration and the temporal correlation hypothesis, *Ann. Rev. Neurosci.* 18 (1995) 555–586.
- [39] D. Terman, D.L. Wang, Global competition and local cooperation in a network of neural oscillators, *Physica D* 81 (1995) 148–176.